# HYBRID FM-POLYNOMIAL PHASE SIGNAL MODELING: PARAMETER ESTIMATION AND PERFORMANCE ANALYSIS

[1] *Fulvio Gini* and [2] *Georgios B. Giannakis*

[1]Dept. "Ingr. dell' Informazione", Univ. of Pisa, via Diotisalvi, 2 I-56126 Pisa, ITALY
Tel: (+39) 50-568550 Fax: (+39) 50-568522 E-mail: gini@iet.unipi.it
[2]Dept. of Electrical Engr., Univ. of Virginia, Charlottesville, VA 22903-2442, U.S.A.
Tel: (804) 924-3659 Fax: (804) 924-8818 E-mail: georgios@virginia.edu

## ABSTRACT

*Parameter estimation for a combination of a polynomial phase signal (PPS) and a frequency modulated (FM) signal is addressed. A novel approach is proposed that allows one to decouple estimation of the FM parameters from that of the PPS parameters, exploiting the properties of the multi-lag High-order Ambiguity Function (ml-HAF). Performance analysis is carried out and Cramer-Rao bounds are compared with simulation results.*

## 1. PROBLEM STATEMENT

The discrete-time model of the hybrid FM-PPS signal of interest is:

$$s(n) = \rho\, e^{j2\pi b \sin(\omega_0 n + \phi_0)}\, e^{j2\pi \sum_{i=0}^{M} a_i n^i / i!}, \tag{1}$$

where: $\{a_i\}_{i=0}^{M}$ are the PPS parameters, $\rho$ denotes a constant (perhaps unknown) amplitude, and $M$ is the PPS order; constant $b > 0$ is the so-called modulation index, $\omega_0$, $\phi_0$ stand for the frequency and initial phase, respectively.

This paper concerns parameter estimation of the hybrid FM-PPS signal in (1) from a finite number of $N$ noisy observations, $\{x(n) = s(n) + v(n)\}_{n=0}^{N-1}$. The additive noise $v(n)$ is assumed stationary, complex white Gaussian, mixing in the sense of [4, p. 25], with zero-mean and variance $\sigma_v^2$. Signals described by (1) are encountered in many engineering applications such as radar, SAR, sonar, acoustics, and optics. When the target is moving, the received signal can be modeled as a discrete-time PPS (see e.g., [10]), and the polynomial coefficients $\{a_i\}$ are related to the kinematics of the moving target [8, p. 403]. The High-order Instantaneous Moment (HIM) and its Fourier transform, the High-order Ambiguity Function (HAF), introduced by Peleg and Porat (see [8, Ch. 12]), have provided a simple albeit sub-optimum algorithm for estimating the PPS coefficients recursively.

Signals arising from moving targets however, cannot always be modeled as a pure PPS. For example, sinusoidal FM signals arise from vibrating targets [5], [12], or, rotating parts of the target [3], [7]. When both of these effects (motion and vibration/rotation) are present, the noise-free backscattered signal obeys (1), and the estimation algorithms proposed in [5] and [11] for a pure sinusoidal FM are no more appropriate.

The main contribution of this paper is to show that the HAF offers a good alternative to the computationally intensive maximum likelihood (ML) approach, even when the observed data cannot be modeled as a pure PPS, but a sinusoidal FM component is also present.

The multi-lag HIM is a nonlinear transformation, originally introduced for continuous-time signals in [1], defined recursively as [2]:

$$\begin{aligned} &x_1(n) = x(n),\ x_2(n;\tau_1) = x_1(n+\tau_1)x_1^*(n-\tau_1),\ \ldots, \\ &x_M(n;\tau_1,\ldots,\tau_{M-1}) = x_{M-1}(n+\tau_{M-1};\tau_1,\ldots,\tau_{M-2}) \\ &\qquad \times x_{M-1}^*(n-\tau_{M-1};\tau_1,\ldots,\tau_{M-2}) . \end{aligned} \tag{2}$$

We term $x_M$ the multi-lag HIM (ml-HIM) because it reduces to the HIM for $\tau_1 = \ldots = \tau_{M-1} = \tau$, [8, Ch. 12], [10]. The ml-HAF is defined as the (generalized) Fourier Series of the ml-HIM:

$$X_M(\alpha;\boldsymbol{\tau}) := \lim_{N\to\infty} \frac{1}{N} \sum_{n=0}^{N-1} x_M(n;\tau_1,\ldots,\tau_{M-1}) e^{-j\alpha n} , \tag{3}$$

where $\boldsymbol{\tau} := [\tau_1\ \tau_2\ \ldots\ \tau_{M-1}]$.

## 2. ESTIMATION ALGORITHMS

Applying the ml-HIM in (2) to the noise-free FM-PPS signal we find:

$$s_M(n;\boldsymbol{\tau}) = \rho^{2^{M-1}} e^{j[\omega_c n + \psi_c + \beta \sin(\omega_0 n + \psi_0)]} , \tag{4}$$

where:

$$\omega_c := 2^M \pi a_M \prod_{m=1}^{M-1} \tau_m ,\quad \psi_c := 2^M \pi a_{M-1} \prod_{m=1}^{M-1} \tau_m , \tag{5}$$

$$\beta := 2^M \pi b \prod_{m=1}^{M-1} \sin(\omega_0 \tau_m) ,\ \psi_0 := \phi_0 + (M-1)\frac{\pi}{2} . \tag{6}$$

Eq. (4) shows that the $M$-th order ml-HIM of a sinusoidal FM signal is still a sinusoidal FM signal, with the same vibration frequency $\omega_0$ but with different modulation index, $\beta$, that is proportional to the original one, $b$.

Being (almost) periodic in $n$, $s_M(n;\boldsymbol{\tau})$ of (4) can be written as a superposition of equally spaced harmonics $\{\omega_c \pm k\omega_0\}$ with amplitudes $\{J_k(\beta)\}$, the $k$th-order Bessel functions of the first kind, [9, p. 311]:

$$s_M(n;\boldsymbol{\tau}) = \rho^{2^{M-1}} \sum_{k=-\infty}^{\infty} J_k(\beta) e^{j[(\omega_c + k\omega_0)n + \psi_c + k\psi_0]} . \tag{7}$$

Because $J_k(\beta)$ vanishes for large $|k|$, [9], there exists a large enough integer $K$ such that most of the energy in $\{J_k(\beta)\}$ is contained in the range $k \in [-K, K]$. It has been shown in [11] that the smallest integer $K$ for which $\sum_{k=-K}^{K} J_k^2(\beta) > 0.99$, is $K \approx \beta + 1$ for $\beta > 1$, whereas $K = 0$ for $\beta \in [0, 0.14)$. For $\beta \in [0.14, 1]$ $K$ is either 1 or 2. Depending on $\beta$, we can

0-8186-8005-9/97 $10.00 © 1997 IEEE

thus approximate the infinite sum in (7) by the partial sum

$$s_M(n;\boldsymbol{\tau}) = \rho^{2^{M-1}} \sum_{k=-K}^{K} J_k(\beta) e^{j[(\omega_c + k\omega_0)n + \psi_c + k\psi_0]} \ , \quad (8)$$

which consists of multi-component constant amplitude tones with harmonic frequencies. Fourier transforming (8), we obtain the ml-HAF as

$$S_M(\alpha;\boldsymbol{\tau}) = \rho^{2^{M-1}} \sum_{k=-K}^{K} J_k(\beta) e^{j(\psi_c + k\psi_0)} \delta(\alpha - \omega_c - k\omega_0) \ , \quad (9)$$

where $\delta(\cdot)$ denotes the Kronecker delta function.

The ml-HAF in (9) peaks at $\{\omega_c + k\omega_0\}_{k=-K}^{K}$. Hence, the vibration frequency $\omega_0$ is given by the distance between successive peaks of $|S_M(\alpha;\boldsymbol{\tau})|$. The position of the central peak is related to the highest order PPS coefficient $a_M$ through $\omega_c$ [c.f. (5)]. Then, making use of (9) one can obtain $\beta$ and $\psi_0$, and subsequently the modulation index $b$ and the phase $\phi_0$, from the values at the peaks.

Sample estimates of $S_M(\alpha;\boldsymbol{\tau})$ are computed from $\{x(n)\}_{n=0}^{N-1}$ as

$$\widehat{S}_M(\alpha;\boldsymbol{\tau}) = \frac{1}{N} \sum_{n=0}^{N-1} x_M(n;\boldsymbol{\tau})\, e^{-j\alpha n}, \quad (10)$$

where $x_M(n;\boldsymbol{\tau})$ is the ml-HIM, and $\widehat{S}_M(\alpha;\boldsymbol{\tau}) = X_M(\alpha;\boldsymbol{\tau})$ is the ml-HAF of the data. Under the stated assumptions on $v(n)$, the estimator in (10) is asymptotically unbiased and consistent in the mean square sense (see [10] for a proof). Once $\widehat{S}_M(\alpha;\boldsymbol{\tau})$ is computed, the parameters of interest can be estimated by substituting $\widehat{S}_M(\alpha;\boldsymbol{\tau})$ for $S_M(\alpha;\boldsymbol{\tau})$ in (9).

We can take advantage of the multiple lags and calculate $X_M$ for $L$ different sets of lags, $\boldsymbol{\tau}_l := [\tau_{1,l} \ \ldots \ \tau_{M-1,l}]$, $l = 1, 2, \ldots, L$, having the same product; i.e., $\prod_{m=1}^{M-1} \tau_{m,l_1} = \prod_{m=1}^{M-1} \tau_{m,l_2}$, $\forall\, l_1, l_2 \in [1, L]$. The product of $L$ ml-HAF amplitudes $\prod_{l=1}^{L} |X_M(\alpha, \boldsymbol{\tau}_l)|$ enhances the desired peaks and reduces noise further than the single ml-HAF [2].

The resulting algorithm is summarized in the following steps.

**Step 1:** Calculate from the data $x_M(n;\boldsymbol{\tau}_l)$, the ml-HIM of order $M$, for each set of lags $\boldsymbol{\tau}_l$, $l = 1, 2, \ldots, L$.

**Step 2:** Estimate the ml-HAF of $s(n)$ using (10).

**Step 3:** Find the peak location of the product ml-HAF, $\prod_{l=1}^{L} |\widehat{S}_M(\alpha, \boldsymbol{\tau}_l)| = \prod_{l=1}^{L} |X_M(\alpha, \boldsymbol{\tau}_l)|$, corresponding to $\{\omega_c + k\omega_0\}_{k=-K}^{K}$ [see also (9)], and collect these values in a $(2K+1) \times 1$ vector $\widehat{\boldsymbol{p}}$.

**Step 4:** Define $\mathbf{A} := [\mathbf{k}\ \mathbf{1}]$, $\widehat{\boldsymbol{\omega}} := [\widehat{\omega}_0\ \widehat{\omega}_c]^T$, and

$$\mathbf{k} := [-K \quad -K+1 \quad \ldots \quad K-1 \quad K]^T,$$

where $\mathbf{1}$ is the vector of ones. Solve the overdetermined linear system $\mathbf{A}\widehat{\boldsymbol{\omega}} \overset{LS}{=} \widehat{\boldsymbol{p}}$, to compute $\widehat{\omega}_0$ and $\widehat{\omega}_c$ as: $\widehat{\boldsymbol{\omega}} = (\mathbf{A}^T\mathbf{A})^{-1}\mathbf{A}^T\widehat{\boldsymbol{p}}$.

**Step 5:** Estimate $a_M$ as:

$$\widehat{a}_M = \widehat{\omega}_c / (2^M \pi \prod_{m=1}^{M-1} \tau_{m,1}) \ . \quad (11)$$

**Step 6:** Estimating $b$ from (10) and (6) requires some care, because (10) is exact only as $N \to \infty$. For finite sample size we find from (1) and (10) that:

$$\widehat{S}_M(\omega_c + k\omega_0;\boldsymbol{\tau}_l) = \rho^{2^{M-1}} \frac{N - 2\sum_{m=1}^{M-1} \tau_{m,l}}{N} \times J_k(\beta_l) e^{j(\psi_c + k\psi_0)} + \textit{noise terms} \ . \quad (12)$$

where $\beta_l := 2^M \pi b \prod_{m=1}^{M-1} \sin(\omega_0 \tau_{m,l})$. To estimate $b$ based on (10), we first find

$$\widehat{J}_k(\beta_l) = \frac{\widehat{S}_M(\widehat{\omega}_c + k\widehat{\omega}_0;\boldsymbol{\tau}_l)}{\rho^{2^{M-1}} (N - 2\sum_{m=1}^{M-1} \tau_{m,l})/N} \ , \ \text{for } k \in [-K, K] \ , \quad (13)$$

and estimate $\beta_l$ as (see also [11]):

$$\widehat{\beta}_l = \frac{2s}{s^2 - 1} \ln \left[ \sum_{k=-K}^{K} \widehat{J}_k(\beta_l)\, s^k \right] \ . \quad (14)$$

Finally, obtain an estimate of $b$ via (6).

**Step 7:** Define:

$$\widehat{\boldsymbol{\psi}} := [\widehat{\psi}_0 \ \ \widehat{\psi}_c]^T, \ \widehat{\Psi}_{k,l} := \arg\{\widehat{S}_M(\widehat{\omega}_c + k\widehat{\omega}_0;\boldsymbol{\tau}_l)\},$$

$$\widehat{\boldsymbol{\Psi}}_l := [\widehat{\Psi}_{-K,l} \ \ldots \ \widehat{\Psi}_{K,l}]^T, \widehat{\boldsymbol{\Psi}} := [\widehat{\boldsymbol{\Psi}}_1^T \ \ldots \ \widehat{\boldsymbol{\Psi}}_L^T]^T,$$

and the $(2M+1)L \times 2$ dimensional matrix $\mathbf{B}$ as:

$$\mathbf{B} := [\mathbf{A}^T \ \ \mathbf{A}^T \ \ \ldots \ \ \mathbf{A}^T]^T \ .$$

Solve the overdetermined linear system $\mathbf{B}\widehat{\boldsymbol{\psi}} \overset{LS}{=} \widehat{\boldsymbol{\Psi}}$ to find $\widehat{\psi}_0$ and $\widehat{\psi}_c$ as: $\widehat{\boldsymbol{\psi}} = (\mathbf{B}^T\mathbf{B})^{-1}\mathbf{B}^T\widehat{\boldsymbol{\Psi}}$.

Then, $\widehat{\phi}_0$ is obtained from $\widehat{\psi}_0$. Now, having estimated $a_M$ and the FM component we can remove it from the data and proceed with the PPS part using techniques described in [10].

As an example, in Fig. 1a we plot the values of the Bessel coefficients $J_k(\beta)$ versus $k$, for $b = 6$, $\omega_0 = 0.0491$, $\tau_1 = 129$. From (5)-(6) we find $\omega_c = 0.5629$ and $\beta = 3.6996$. The values of the other parameters can be found in the Example 2, Section 4. As expected, the coefficients become negligible for $|K| > 5$ in (7), confirming that $K \approx \beta + 1$. In Fig. 1b the ml-HAF $X_2(\alpha;\tau_1)$ is plotted for $\alpha \in [0, 1]$, $SNR := \rho^2/\sigma_v^2 = 16\ dB$, and $N = 1{,}024$. From the location (and value) of the peaks we derive our estimates.

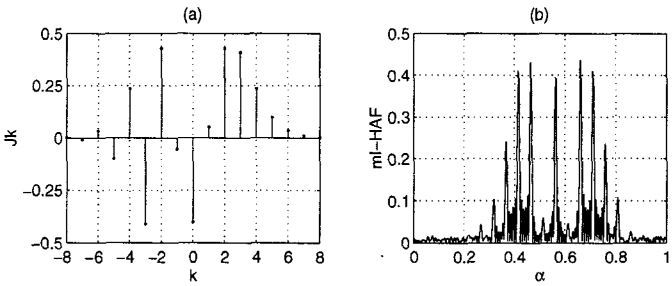


**Figure 1.** (a) Bessel coefficients $J_k(\beta)$ vs. $k$, for $\beta = 3.6996$. (b) $X_2(\alpha;\tau_1)$ vs. $\alpha$, for $SNR = 16\ dB$ and $N = 1{,}024$.

**Narrowband FM.** According to Carson's rule the bandwidth of an FM signal is approximately $2\omega_0(1 + \beta)$, [9, p. 313]. We will refer to the case discussed so far, for general $\beta$, as the wideband FM (WBFM). Expanding $\exp[j\beta \sin(\omega_0 n + \psi_0)]$ in Taylor series we find:

$$e^{j\beta \sin(\omega_0 n + \psi_0)} = \sum_{k=0}^{\infty} \frac{[j\beta \sin(\omega_0 n + \psi_0)]^k}{k!} \quad (15)$$

If $\beta$ is small enough, we can truncate the series expansion as follows:

$$
\begin{aligned}
e^{j\beta\sin(\omega_0 n+\psi_0)} \approx & \\
& 1 + j\beta\sin(\omega_0 n + \psi_0) - \frac{1}{2}\beta^2\sin^2(\omega_0 n + \psi_0) \\
= & \; 1 - \frac{\beta^2}{4} + j\beta\sin(\omega_0 n + \psi_0) - \frac{\beta^2}{4}\cos(2\omega_0 n + 2\psi_0).
\end{aligned}
$$

A value of $\beta < 1$ is sufficient to guarantee that the second order approximation is valid. We will refer to the case of $\beta < 1$ as narrowband FM (NBFM). Using this approxmation in (8) we obtain:

$$
\begin{aligned}
S_M(\alpha;\tau) \approx & \; \rho^{2^{M-1}}[-\frac{\beta^2}{8}\, e^{j(\psi_c-2\psi_0)}\delta(\alpha-\omega_c+2\omega_0) \\
+ & \; \frac{\beta}{2}\, e^{j(\psi_c-\psi_0)}\delta(\alpha-\omega_c+\omega_0) + (1-\frac{\beta^2}{4})\, e^{j\psi_c}\delta(\alpha-\omega_c) \\
+ & \; \frac{\beta}{2}\, e^{j(\psi_c+\psi_0)}\delta(\alpha-\omega_c-\omega_0) \\
- & \; \frac{\beta^2}{8}\, e^{j(\psi_c+2\psi_0)}\delta(\alpha-\omega_c-2\omega_0)], \qquad (16)
\end{aligned}
$$

which makes estimation of $\beta$ from the amplitude of the peaks easier. Note that the bandwidth of the signal in (16) is $4\omega_0$ as predicted by Carson's rule (with $\beta = 1$). The estimation algorithm is obtained by modifying Step 6 as follows:

**Step 6 (NBFM):** Exploit (15) to obtain different estimates of $\beta$ as:

$$
\begin{aligned}
\widehat{\beta}_{0,l} &= 2\sqrt{1 - \frac{|\widehat{S}_M(\widehat{\omega}_c;\tau_l)|}{\rho^{2^{M-1}}(N - 2\sum_{m=1}^{M-1}\tau_{m,l})/N}}\,, \\
\widehat{\beta}_{1,l} &= \frac{|\widehat{S}_M(\widehat{\omega}_c+\widehat{\omega}_0;\tau_l)| + |\widehat{S}_M(\widehat{\omega}_c-\widehat{\omega}_0;\tau_l)|}{\rho^{2^{M-1}}(N - 2\sum_{m=1}^{M-1}\tau_{m,l})/N}, \qquad (17) \\
\widehat{\beta}_{2,l} &= 2\sqrt{\frac{|\widehat{S}_M(\widehat{\omega}_c+2\widehat{\omega}_0;\tau_l)| + |\widehat{S}_M(\widehat{\omega}_c-2\widehat{\omega}_0;\tau_l)|}{\rho^{2^{M-1}}(N - 2\sum_{m=1}^{M-1}\tau_{m,l})/N}}\,,
\end{aligned}
$$

and then take their mean, $\widehat{\beta} = 1/(3L)\sum_{l=1}^{L}\sum_{i=0}^{2}\widehat{\beta}_{i,l}$. Finally, $\widehat{b}$ is derived by inserting $\widehat{\beta}$ in (6). The other steps remain unchanged. It is worth observing that because $\beta = 2^M\pi b\prod_{m=1}^{M-1}\sin(\omega_0\tau_m)$, it is possible to select the lags $\tau$ in order to have $\beta < 1$. This allows estimation of $\beta$ using the second-order approximation (16).

## 3. PERFORMANCE EVALUATION

Consider the PPS-FM model in (1) and denote the parameter vector as $\boldsymbol{\theta}$. To avoid numerical problems in the inversion of the Fisher information matrix, it is useful to define $\boldsymbol{\theta}$ as follows:

$$\boldsymbol{\theta} := [N^0 a_0 \; \ldots \; N^M a_M \;\; b \;\; N\omega_0 \;\; \phi_0]^T. \qquad (18)$$

If $\widehat{\boldsymbol{\theta}}$ is an unbiased estimator of $\boldsymbol{\theta}$, then it must satisfy $\mathrm{cov}(\widehat{\boldsymbol{\theta}}) \geq \mathbf{J}^{-1}$, where $\mathbf{J}$ is the so-called Fisher information matrix (FIM). As a first step towards deriving the CRLBs, let us write the observed data in vector form as $\mathbf{x} = \mathbf{s}(\boldsymbol{\theta}) + \mathbf{v}$, where $[\mathbf{x}]_n := x(n)$, $n = 0, 1, \ldots, N-1$; similar definitions apply to $\mathbf{s}(\boldsymbol{\theta})$ and $\mathbf{v}$. Due to the assumptions on $v(n)$, we have that $\mathbf{x}$ is an $N \times 1$ complex Gaussian circular vector, with mean value $E\{\mathbf{x}\} = \mathbf{s}$ and covariance matrix $E\{\mathbf{x}\mathbf{x}^H\} = \sigma_v^2\mathbf{I}$, where $^H$ denotes conjugate transpose, and $\mathbf{I}$ is an $N \times N$ identity matrix. Calculation of the FIM for a vector of correlated complex Gaussian observations is carried out in [6, Ch. 3], and in our case it produces for the $(i,j)$th entry:

$$J_{ij} = \frac{2}{\sigma_v^2}\Re\left\{\frac{\partial\mathbf{s}^H(\boldsymbol{\theta})}{\partial\theta_i}\frac{\partial\mathbf{s}(\boldsymbol{\theta})}{\partial\theta_j}\right\}. \qquad (19)$$

The CRLBs are obtained from the diagonal elements of $\mathbf{J}^{-1}$, which we denote as $CRLB(\theta_i) = [\mathbf{J}^{-1}]_{ii}$. Inserting $s(n)$ of (1) in (19) and taking partial derivatives, we obtain the elements of the FIM. Evaluation of $J_{ij}$ is not difficult but tedious. Skipping the details, we found:

$$
\begin{aligned}
J_{a_i,a_m} &= \frac{8\pi^2\rho^2}{i!m!\,\sigma_v^2}\sum_{n=0}^{N-1}\left(\frac{n}{N}\right)^{i+m}, \; 0 \leq i,m \leq M, \qquad (20) \\
J_{b,b} &= \frac{8\pi^2\rho^2}{\sigma_v^2}\sum_{n=0}^{N-1}\sin^2(\omega_0 n+\phi_0)\,, \qquad (21) \\
J_{\omega_0,\omega_0} &= \frac{8\pi^2\rho^2 b^2}{\sigma_v^2}\sum_{n=0}^{N-1}\left(\frac{n}{N}\right)^2\cos^2(\omega_0 n+\phi_0)\,, \qquad (22) \\
J_{\phi_0,\phi_0} &= \frac{8\pi^2\rho^2 b^2}{\sigma_v^2}\sum_{n=0}^{N-1}\cos^2(\omega_0 n+\phi_0)\,, \qquad (23) \\
J_{a_i,b} &= \frac{8\pi^2\rho^2}{i!\,\sigma_v^2}\sum_{n=0}^{N-1}\left(\frac{n}{N}\right)^i\sin(\omega_0 n+\phi_0)\,, \qquad (24) \\
J_{a_i,\omega_0} &= \frac{8\pi^2\rho^2 b}{i!\,\sigma_v^2}\sum_{n=0}^{N-1}\left(\frac{n}{N}\right)^{i+1}\cos(\omega_0 n+\phi_0)\,, \qquad (25) \\
J_{a_i,\phi_0} &= \frac{8\pi^2\rho^2 b}{i!\,\sigma_v^2}\sum_{n=0}^{N-1}\left(\frac{n}{N}\right)^i\cos(\omega_0 n+\phi_0)\,, \qquad (26) \\
J_{b,\omega_0} &= \frac{4\pi^2\rho^2 b}{\sigma_v^2}\sum_{n=0}^{N-1}\left(\frac{n}{N}\right)\sin(2\omega_0 n+2\phi_0)\,, \qquad (27) \\
J_{b,\phi_0} &= \frac{4\pi^2\rho^2 b}{\sigma_v^2}\sum_{n=0}^{N-1}\sin(2\omega_0 n+2\phi_0)\,, \qquad (28) \\
J_{\omega_0,\phi_0} &= \frac{8\pi^2\rho^2 b^2}{\sigma_v^2}\sum_{n=0}^{N-1}\left(\frac{n}{N}\right)\cos^2(\omega_0 n+\phi_0)\,. \qquad (29)
\end{aligned}
$$

Equations (20)-(29) allow the exact numerical evaluation of the FIM, but it is not clear how the parameters affect the bounds. However, a large sample approximation can be derived by regarding the sums as an Euler approximation of the integral, $\sum_{n=0}^{N-1} f(n) \approx \int_0^N f(t)dt$. With this in mind, we obtain:

$$
\begin{aligned}
J_{a_i,a_m} &= \frac{8\pi^2\rho^2}{(i+m+1)i!m!\,\sigma_v^2}, \; 0 \leq i,m \leq M, \\
J_{b,b} &= \frac{4\pi^2\rho^2}{\sigma_v^2}\left[N - \frac{\sin(2\omega_0 N+2\phi_0)-\sin(2\phi_0)}{2\omega_0}\right], \\
J_{\omega_0,\omega_0} &= \frac{4\pi^2\rho^2 b^2}{\sigma_v^2}\left[\frac{N}{3} + \frac{\sin(2\omega_0 N+2\phi_0)}{2\omega_0}\right], \\
J_{\phi_0,\phi_0} &= \frac{4\pi^2\rho^2 b^2}{\sigma_v^2}\left[N + \frac{\sin(2\omega_0 N+2\phi_0)-\sin(2\phi_0)}{2\omega_0}\right],
\end{aligned}
$$

$$
\begin{aligned}
J_{a_0,b} &= -\frac{8\pi^2\rho^2}{i!\ \sigma_v^2}\cdot\frac{\cos(\omega_0 N+\phi_0)-\cos(\phi_0)}{\omega_0},\\
J_{a_i,b} &= -\frac{8\pi^2\rho^2}{i!\ \sigma_v^2}\cdot\frac{\cos(\omega_0 N+\phi_0)}{\omega_0},\ 1\le i\le M,\\
J_{a_i,\omega_0} &= \frac{8\pi^2\rho^2 b}{i!\ \sigma_v^2}\cdot\frac{\sin(\omega_0 N+\phi_0)}{\omega_0},\\
J_{a_0,\phi_0} &= \frac{8\pi^2\rho^2 b}{\sigma_v^2}\cdot\frac{\sin(\omega_0 N+\phi_0)-\sin(\phi_0)}{\omega_0},\\
J_{a_i,\phi_0} &= \frac{8\pi^2\rho^2 b}{i!\ \sigma_v^2}\cdot\frac{\sin(\omega_0 N+\phi_0)}{\omega_0},\ 1\le i\le M,\\
J_{b,\omega_0} &= -\frac{4\pi^2\rho^2 b}{\sigma_v^2}\cdot\frac{\cos(2\omega_0 N+2\phi_0)}{2\omega_0},\\
J_{b,\phi_0} &= -\frac{4\pi^2\rho^2 b}{\sigma_v^2}\cdot\frac{\cos(2\omega_0 N+2\phi_0)-\cos(2\phi_0)}{2\omega_0},\\
J_{\omega_0,\phi_0} &= \frac{2\pi^2\rho^2 b^2}{\sigma_v^2}\left[N+\frac{\sin(2\omega_0 N+2\phi_0)}{2\omega_0}\right].
\end{aligned}
$$

In Fig. 2 the CRLBs of the FM and PPS parameters are reported for $SNR = 12\ dB$, $b = 0.05$, $\omega_0 = 0.015$, and $\phi_0 = 0$. The solid and dashed lines refer to the exact and approximate CRLBs, respectively. The dashdotted lines refer to the exact CRLBs when only FM or only PPS parameters are present (let us call them marginal CRLBs). As we see, asymptotic behavior is reached at about $N = 1000$. The effect of coupling beetwen the PPS and the FM parameters is evident by comparing the plots with solid and dashdotted lines. The results show that for $N > 1000$ the coupling tends to be negligible.

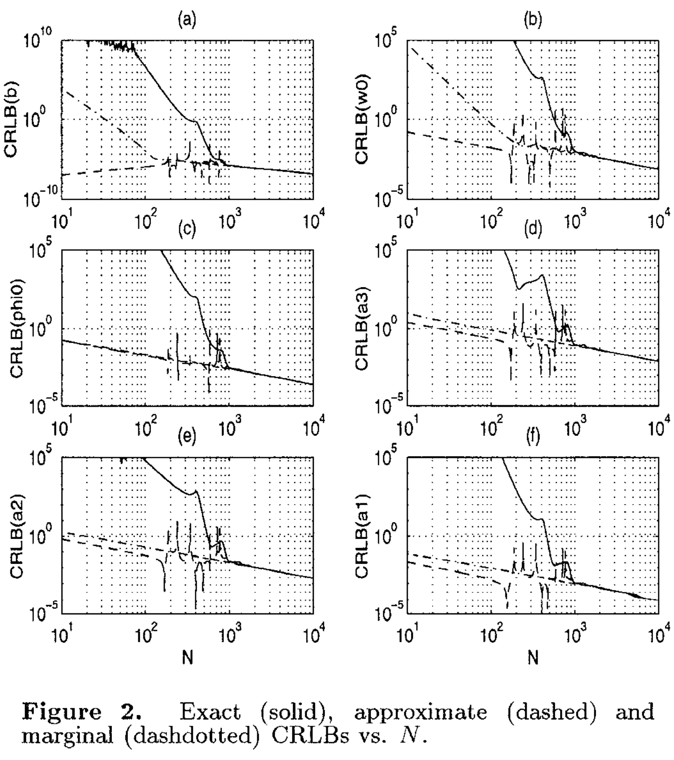


**Figure 2.** Exact (solid), approximate (dashed) and marginal (dashdotted) CRLBs vs. $N$.

To illustrate and evaluate the various parameter estimation algorithms discussed so far, we simulated numerically the performance by Monte Carlo experiments and we compared them with the CRLBs.

**Example 1:** Narrowband FM signal and $3^{rd}$-order PPS. We first generated $N = 2,048$ samples according to (1), with parameters: $\rho = 1$, $b = 0.05$, $\omega_0 = 0.015$, $\phi_0 = 0$, $a_0 = 0$, $a_1 = 0.25$, $a_2 = 1.3889 \cdot 10^{-3}$, $a_3 = 1.3022 \cdot 10^{-5}$. The noise variance $\sigma_v^2$ was set to obtain the desired signal-to-noise ratio, defined as $SNR := \rho^2/\sigma_v^2$. The sets of lags in the product ml-HAF were: $(\tau_{1,l}, \tau_{2,l}) = (60,60), (72,50), (75,48), (80,45), (90,40)$, and $(100,36)$, so that $\tau_{1,l}\cdot\tau_{2,l} = 3600$, for $l = 1,\cdots,6$; consequently $\omega_c = 1.1782$ and $\beta_l = 0.7711, 0.7555, 0.7476, 0.7319, 0.6923, 0.6445$, respectively. Note that all of them are less than one, so the second-order approximation is valid. All FFT operations were carried out by zero-padding to $N_{zp} = 2^{16}$ points so that the frequency bins were small enough to allow accurate estimation of the peaks' location.

In Fig. 3 we show the mean square errors (mse) of the estimates versus $SNR$, obtained from 400 independent Monte Carlo runs (in each run we generated $N = 2,048$ samples). The solid lines refer to the approximate CRLBs ($CRLB(\omega_0)$ and $CRLB(a_m)$ were properly scaled by $N^2$ and $N^{2m}$, respectively); the dashed lines correspond to the mse obtained assuming known amplitude $\rho$; and the dashdotted lines refer to the case where $\rho$ is unknown and is estimated using the following algorithm based on fourth order cumulants:

$$
\widehat{\rho} = \left[2\left(\frac{1}{N}\sum_{n=0}^{N-1}|x(n)|^2\right)^2 - \frac{1}{N}\sum_{n=0}^{N-1}|x(n)|^4\right]^{1/4}. \quad (30)
$$

Unbiasedness and mean square consistency follow from the mixing conditions assumed to be satisfied for $v(n)$; the proof is standard and is not reported here.

In the range of $SNRs$ investigated, no sensible difference was observed, between the two cases (known $\rho$ and unknown $\rho$), except for the mse of $\widehat{b}$. We also note that the mse's of $\widehat{a}_3$ and $\widehat{a}_2$ are not very close to the bounds. The reason is related to the amount of zero-padding [10]. Similar results have been obtained for the other parameters, but are not reported here due to space limitations. Finally, in Fig. 4 we report the mse's and the exact CRLBs for the estimators of $b$ and $\omega_0$ versus $N$. As expected, when $CRLB(\omega_0)$ drops below $10^{-10}$ the mse is no more able to track the bound, due to the limited FFT resolution.

**Example 2:** Wideband FM signal and $2^{nd}$-order PPS. Here, we generated $N = 1,024$ samples of the FM-PPS process with second-order polynomial phase, and parameters given by: $b = 6$, $\omega_0 = 0.0491$, $\phi_0 = 0$, $a_0 = 0.5$, $a_1 = 0.1$, $a2 = 3.4722 \cdot 10^{-4}$, and $\tau_1 = 129$, so $\omega_c = 0.5629$ and $\beta = 3.6996$. The modulation index was estimated according to the method reported in (14), proposed in [11]. Note that $\beta > 1$, so we cannot use (17).

Tables I and II show biases and variances of the estimates for the $SNR = 16\ dB$ (first two rows) and $8\ dB$ (last two rows), obtained from 400 independent Monte Carlo runs ($N = 1,024$ samples per each run). As we see from Table II, low SNR increases the variance of $b$. Even if the estimator (14) guarantees reliable estimates of the modulation index for a pure FM tone observed in additive white Gaussian noise (see [11]), when it is applied to the "data" $x_M(n;\tau_l)$ all the cross-terms between $s(n)$ and $v(n)$, present in the ml-HIM of $x(n)$, contribute to the disturbance term, which consequently can no longer be considered white or Gaussian process. This seems to have deleterious effects on the performance of (14), as shown in Table II.

A possible remedy is to use the estimate $\omega_0$ to select a new set of lags in such a way that $\beta < 1$, and then estimate $b$ as in Step 6. We repeated the simulations, this time with $\tau_1 = 256$, so that $\beta = 0.2435$, and we obtained

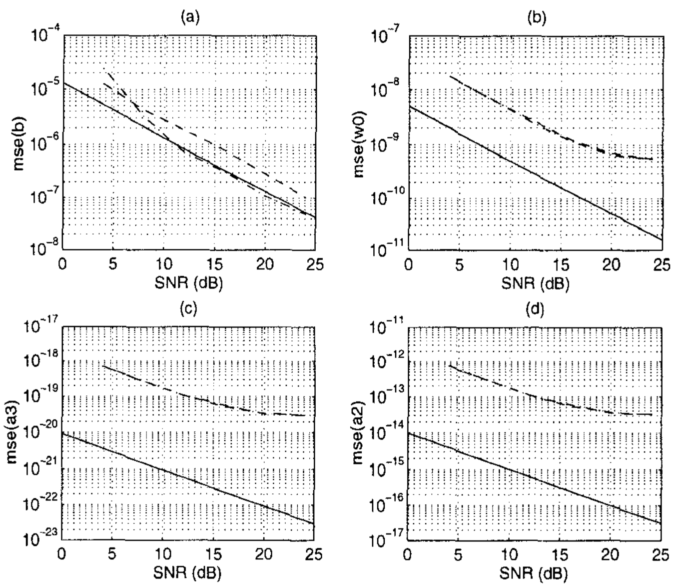


**Figure 3.** Mean square error for known $\rho$ (dashed), unknown $\rho$ (dashdotted), and CRLBs (solid) vs. $SNR$.

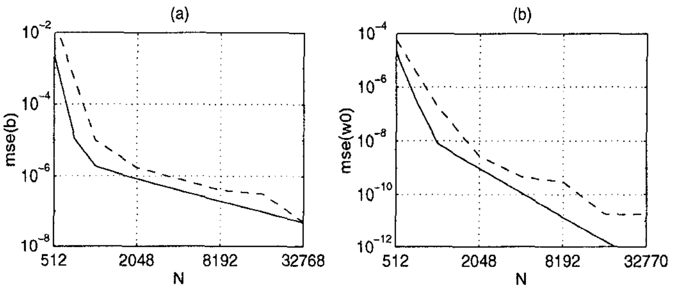


**Figure 4.** Mean square error (dashed) and CRLBs (solid) vs. $N$.

bias$(\widehat{b}) = 0.1384$, var$(\widehat{b}) = 0.6407$ for $SNR = 16\ dB$, and bias$(\widehat{b}) = 0.1469$, var$(\widehat{b}) = 3.0400$ for $SNR = 8\ dB$. The accuracy improvement (at least for the low $SNR$ case) is now noticeable.

Table I - PPS parameters ($SNR = 16\ dB$ and $8\ dB$)

| | $\widehat{a_2}$ | $\widehat{a_1}$ | $\widehat{a_0}$ |
|---|---|---|---|
| Bias | $-1.8236 \cdot 10^{-8}$ | 0.0 174 | -0.2938 |
| Var | $2.327 \cdot 10^{-15}$ | 0.0028 | 0.0376 |
| Bias | $-4.3700 \cdot 10^{-7}$ | -0.0226 | -0.4019 |
| Var | $5.6254 \cdot 10^{-13}$ | 0.0276 | 0.0765 |

Table II - FM parameters ($SNR = 16\ dB$ and $8\ dB$)

| | $\widehat{b}$ | $\widehat{\omega_0}$ | $\widehat{\psi_0}$ |
|---|---|---|---|
| Bias | $-1.3579$ | $-1.9890 \cdot 10^{-5}$ | 0.0574 |
| Var | 0.0460 | $2.7497 \cdot 10^{-10}$ | $4.7490 \cdot 10^{-5}$ |
| Bias | $-4.1559$ | $-7.6639 \cdot 10^{-5}$ | 0.0549 |
| Var | $1.1172 \cdot 10^4$ | $3.1892 \cdot 10^{-8}$ | 0.0106 |

## 4. CONCLUSIONS

Parameter estimation of a class of nonstationary complex signals whose phase can be modeled as a superposition of a polynomial term and a sinusoidal frequency modulated term was addressed. Previously proposed methods for estimating the FM parameters (and in particular the modulation index) do not include PPS components, and, vice-versa, the standard approach based on the HAF for PPS parameter estimation cannot work when the FM component is present. The proposed method handles the more general scenario of hybrid FM-PPS signals exploiting the properties of the multi-lag HAF. This approach allows one to decouple estimation of the FM parameters from that of the PPS, with a noticeable reduction in computational complexity. The redundancy offered by the multi-lags was also used to reduce the FM term to a narrowband process, and thereby improves the accuracy of the modulation index estimation. The exact Fisher information matrix for the FM-PPS parameters was also derived along with an asymptotic form of the CRLBs. Computer simulations were carried out to compare the performance of the proposed methods with the relevant CRLBs. The model adopted herein is potentially useful for practical radar/sonar modeling and target classification.

## REFERENCES

[1] S. Barbarossa, "Detection and estimation of the instantaneous frequency of polynomial phase signals by multilinear time-frequency representations," *Proc. of IEEE-SP Workshop on Higher Order Statistics*, pp. 168-172, Lake Tahoe, CA, June 1993.

[2] S. Barbarossa, A. Porchia, and A. Scaglione, "Multiplicative multilag higher-order ambiguity function," *Proc. of Int. Conf. on Acoustics, Speech, and Signal Processing*, vol. 5, pp. 3022-3025, Atlanta, GA, May 1996.

[3] M. R. Bell, R. A. Grubbs, "JEM modeling and measurement for radar target identification," *IEEE Trans. on AES*, vol. 29, pp. 73-87, Jan. 1993.

[4] D. R. Brillinger, *Time Series: Data Analysis and Theory*, Holden-day Inc., San Francisco, 1981.

[5] S.-R. Huang, R. M. Lerner, and K. J. Parker, "On estimating the amplitude of harmonic vibration from the Doppler spectrum of reflected signals", *J. of the Acoust. Soc. Am.*, vol. 88, pp. 2702-2712, Dec. 1990.

[6] S. M. Kay, *Fundamentals of Statistical Signal Processing: Estimation Theory*, Prentice Hall, NJ, 1993.

[7] S. Palumbo, S. Barbarossa, A. Farina, and M. R. Toma, "Classification techniques of radar signals backscattered by helicopter blades", *Proc. of Int. Symp. on Digital Signal Processing*, London, UK, July, 1996.

[8] B. Porat, *Digital Processing of Random Signals, Theory & Methods*, Prentice Hall, NJ, 1994.

[9] F. G. Stremler, *Introduction to Communication Systems*, third edition, Addison Wesley, 1990.

[10] G. T. Zhou, G. B. Giannakis and A. Swami, "On polynomial phase signals with time-varying amplitudes," *IEEE Trans. on Signal Processing*, vol. 44, pp. 848-861, April 1996.

[11] G. T. Zhou and G. B. Giannakis, "Parameter estimation of FM signals using cyclic statistics," *IEEE-SP Intl. Symposium on Time-Frequency and Time-Scale Analysis*, pp. 248-251, Philadelphia, Pennsylvania, October 25-28, 1994.

[12] J.-E. Wilbur and R. J. McDonald, "Nonlinear analysis of cyclically correlated spectral spreading in modulated signals", *J. of the Acoust. Soc. of America*, vol. 92, pp. 219-230, July 1992.

**Acknowledgements:** The authors would like to thank Profs. G. Tong Zhou and Alfonso Farina for useful comments. The work in this paper was supported by ONR Grant No. N00014-93-1-0485.